

## SYSTEMATIC TESTING OF THE FATIGUE PERFORMANCE OF SUBMERGED SMALL-SCALE GROUTED JOINTS

Peter Schaumann

ForWind – Center for Wind Energy Research,  
 Institute for Steel Construction,  
 Leibniz University Hannover,  
 Hannover, Germany

Alexander Raba

ForWind – Center for Wind Energy Research,  
 Institute for Steel Construction,  
 Leibniz University Hannover,  
 Hannover, Germany

### ABSTRACT

With an increasing demand for renewable energy, offshore wind farms become more and more important. Within the next 15 years the German government intends to realize offshore wind farms with a capacity of 15 GW of electrical energy. This corresponds to approximately 3000 to 4000 new turbines.

The grouted joint is a common structural detail for the connection between substructure and foundation piles in offshore wind turbine structures. For lattice substructures such as jackets, the connection is located just above the seabed and is permanently surrounded by water.

Prior investigations by Schaumann et al. showed that the surrounding water may have an impact on the fatigue performance of grouted joint specimens. Thus far, very few results of submerged fatigue tests on grouted joint specimens are published and their statistical reliability is insecure.

Within this paper, 24 individual test results are presented. Regarding test parameters, the focus is set on two different applied load levels, two different loading frequencies and two different grout materials. All parameters are varied in a factorial experiment and are statistically evaluated.

The evaluation shows that load level and loading frequency have a significant effect on the fatigue performance of the connection. Moreover, both effects are significantly correlated. For the used grout materials no significant impact is visible, which can be explained by their similarity regarding mechanical properties and micro structure. Furthermore, the mean displacement and the stiffness degradation of the specimens during fatigue tests are discussed in detail in the paper.

In conclusion, previously published results on the fatigue performance of submerged small scale grouted joint specimens can be confirmed. Load level as well as loading frequency can be stated as most relevant parameters for the fatigue performance.

### 1 INTRODUCTION

Offshore wind turbines (OWT), consisting of rotor, nacelle and tower, are founded on substructures standing in water. Offshore wind farms in Germany are mainly located in water depths of 30 m and deeper. For these water depths lattice substructures such as jackets (cf. Figure 1) are an optional type of construction. These substructures are founded on steel piles which are driven into the seabed. The connection between substructure and foundation pile is realized by a grouted joint.

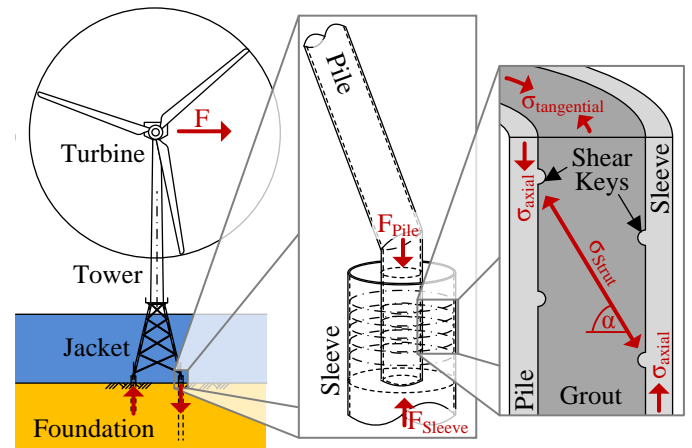


Figure 1: OWT founded on a jacket substructure, close-up of a grouted joint and its cross section and load bearing behaviour

A grouted joint consists of a steel tube with a smaller diameter (pile) which is plugged into a steel tube with a larger diameter (sleeve) (cf. Figure 1). A high strength grout material is filled in the resulting annulus between the steel tubes. The surfaces of the steel tubes facing towards the grout are equipped with weld beads (shear keys). This profiling creates a defined interlocking between steel and grout and therefore, a defined load transfer. Since the connections between foundation

piles and jacket substructure are located close to the seabed, grouted joints are permanently submerged.

Wind and wave loads, acting on the turbine and the substructure, lead to alternating bending loads within the whole structure. Due to the large footprint of lattice substructures, these bending loads are split into axial force couples (cf. Figure 1). Each foundation pile is subjected to alternating axial loads. Therefore, grouted joints in these substructures are predominantly axial loaded.

The axial load is transferred from pile to sleeve via the grout annulus. Between two shear keys a compression strut evolves in the grout at an angle  $\alpha$  between  $\sim 30^\circ$  and  $\sim 60^\circ$  (cf. Lamport [1] and Figure 1). The horizontal part of this compression strut is carried by tangential stresses in the steel tubes. Transverse to the compression strut, tensile stresses occur.

Due to alternating loads, causing high stress ranges in the grout section, fatigue is generally decisive for the connection's design. Current standards for the design of OWT substructures provide design regulations for the fatigue limit state (FLS). But as described in detail by Schaumann et al. [2], these regulations show several weaknesses for the application on current designs.

For example in the ISO 19902 standard [3] a fatigue limit is assumed to be valid for the connection. As a result the fatigue strength is independent from the number of applied load cycles  $N$ . These design regulations are based on investigations by Billington et al. [4] and Harwood et al. [5]. Drawbacks of these regulations are also discussed by Billington et al. [6]. All of these tests are conducted on grouted joint specimens with shear keys and in dry ambient conditions. Therefore, the applicability of these results for submerged grouted joints is questionable.

The DNV-OS-J101 offshore standard [7] provides a significantly more progressive approach. The fatigue strength has to be calculated with an SN-curve which depends on the ambient conditions. But as stated by Schaumann et al. [2] the SN-curve for wet ambient conditions is based on few pure grout material tests.

Previous investigations by Waagaard [8,9], Nishiyama [10], Nygaard [11] and Soerensen [12] showed an influence of the surrounding water on the fatigue performance of submerged material and reinforced concrete specimens. As shown in Figure 2, in all tests water reduced the number of endurable load cycles  $N$  for the specimens.

From the given description of grouted joints and the state of knowledge about the connection, the following question can be derived. Is there a significant influence of the surrounding water on the fatigue performance of submerged grouted joints? Finding an answer to this question is part of the research project 'GROWup – Grouted Joints for Offshore Wind Energy Converters under reversed axial loadings and up scaled thicknesses' (funding sign: 0325290) funded by the German Federal Ministry for Economic Affairs and Energy (BMWi). The research partners are Institute for Steel Construction (IfS) and Institute of Building Materials Science (IfB), both residents at the Leibniz University Hannover, Germany.

First results of submerged grouted joint fatigue tests were published by Schaumann et al. in 2013 [13] and 2014 [2]. The published results showed an influence of the ambient condition (AC) as well as the applied maximum load  $F_{max}$  and the loading frequency  $f$  on the fatigue performance of the specimens. In general, the contact interface between steel and grout opens when the grout is deformed by applied loads. Subsequently, the surrounding water invades into the contact interface. Due to the mechanical movement of the steel tubes, the water is pumped through the interface. High water overpressure and local load application of the shear keys lead to cracking of the grout. Subsequently, the loosened grout material is flushed out of the connection and the grout section loses volume. In total, this process leads to a stiffness degradation of the connection.

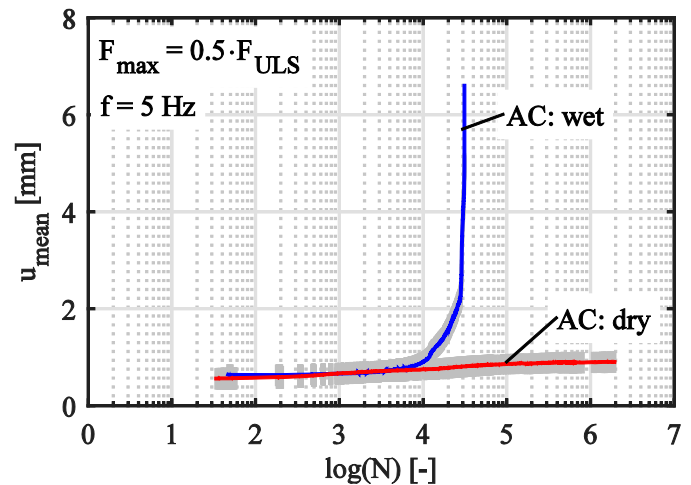


Figure 2: Deformation evolution of small scale grouted joint specimen loaded in dry and wet ambient conditions, from [13]

Since these results are based on very few individual tests without any repetition, they lack of statistical reliability. Within the following, these prior test results will be verified by a systematic and statistically evaluable factorial design procedure.

## 2 MATERIALS AND METHODS

### 2.1 Small scale specimen

Within the research project 'ForWind' [14] a small scale specimen was developed (cf. Figure 3). The main objective was to investigate the behaviour of different filling materials under the multiaxial stress state, which is typical for grouted joints. To realize a failure of the filling material and avoid buckling or yielding of the steel tubes, the tubes have a relatively low slenderness compared to real connections. Also a profiling of the steel surfaces is realized. Rectangular shear keys are turned out of the tube's surface. With this production procedure a high reproducibility of the specimen's geometry can be realized. For the filling process the steel parts are put on a plastic plug. This plug seals the lower end of the grout annulus and secures a centric position of the pile.

This small scale specimen geometry was already used in prior investigations by Anders [15], Schaumann et al. [16], Lochte-Holtgreven [17] and Wilke [18]. Therefore, numerous results are available for comparison with the new test results.

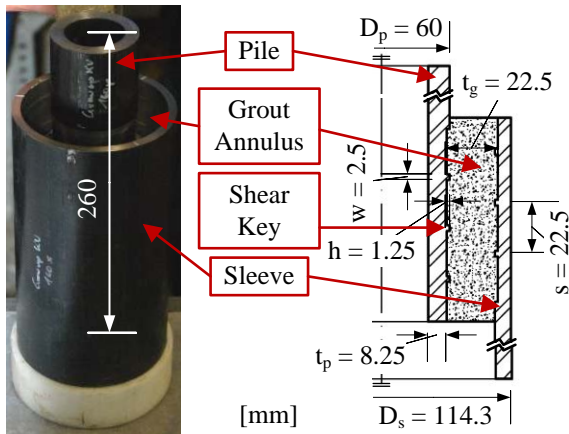


Figure 3: Picture and geometric dimensions of the small scale grouted joint specimen

## 2.2 Fatigue test rig and measurement data

The small scale specimens are tested in ultimate limit state ULS tests (cf. [2]) as well as fatigue performance tests (cf. Figure 4). The fatigue tests are conducted with a servo-hydraulic cylinder with a capacity of  $F_{max} = \sim 320$  kN dynamic loading up to a loading frequency of  $f = 10$  Hz. The hydraulic cylinder is equipped with an axial hinge to exclude bending loading due to eccentric positioning of the specimen. Moreover, the cylinder includes a load cell to measure the load applied to the specimen. Due to the test rig's properties, only pulsating compression tests can be realized. The specimen is located in a water basin, which allows for dry and wet (fresh water) ambient conditions.

In addition to the load cell in the hydraulic cylinder, the deformation of the specimen is measured with displacement lasers. Three lasers are positioned around the specimen at  $0^\circ$ ,  $120^\circ$ ,  $240^\circ$  angles and are oriented to the top of the load

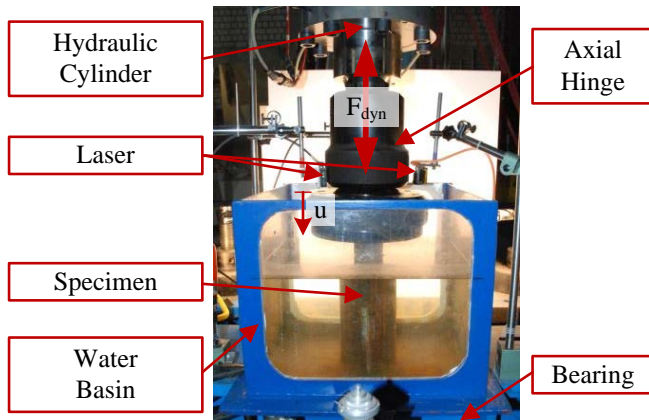


Figure 4: Testing rig for the submerged fatigue tests

application plate of the hydraulic cylinder. The lasers are mounted to monopods, which stand on the base bearing of the water basin. As a result, the mean value of the three laser signals shows the relative displacement of load application plate, specimen and water basin floor. During the fatigue tests the minimum and maximum load  $F$  and displacement  $u$  per load cycle  $N$  is detected and stored. Other parameters are not controlled.

## 2.3 Grout materials

To investigate the influence of different grout material strengths, two commercial grout products from different manufacturers are chosen for the tests. Grout material 1 has, according to the manufacturer, a uniaxial compressive strength of  $90$  N/mm<sup>2</sup> (cf. Figure 5). Grout material 2 has a uniaxial compressive strength of  $140$  N/mm<sup>2</sup> which is about 1.5 times higher than for material 1. Both materials are fine grain grouts with a maximum aggregate size of  $5$  mm. The mixture consists of about  $8\%$  of water.

The grouted joint specimens are filled with grout material and covered with foil in order to slow down the drying process and reduce shrinkage of the grout. After 24 hours the plastic plug (cf. Section 2.1) is removed and the specimens are stored in a fresh water filled water basin at room temperature until they are tested. The first tests are carried out after at least 28 days of curing. The storing in the water basin ensures a minimized shrinkage of the grout material.

During the production of the grouted joint specimens, the quality of the grout material is monitored by the Institute for Building Materials Science (IfB). Besides slump tests on the day of production the material's strength and stiffness at an age of 28 days is determined (cf. Figure 5). Three batches per material were produced.

## 2.4 Test parameters

According to prior investigations [2], three parameters can be determined to have an influence on the fatigue performance of grouted joints. These parameters are ambient condition AC (dry/wet), maximum compressive load  $F_{max}$  and loading frequency  $f$ . Since the prior investigations were carried out for one filling material only, the grout material is added to the parameters of interest.

To determine the significance of these parameters the usual experimental approach of one factor at a time is time consuming and costly. A more effective and still statistically fail-safe approach is the factorial experiment according to rules of Design of Experiments (DoE) [19]. A factorial experiment gives the opportunity to investigate several parameters or factors by a minimum amount of tests. For the evaluation of the test results, all results are included in the statistical assessment of each parameter. Besides assessing the effect of each parameter, the factorial experiment allows for assessing the interaction between the parameters.

Investigations by Lochte-Holtgreven [17] with the same specimen geometry showed, that for dry AC no fatigue degradation of the grouted joint specimens occurs when  $F_{max}$  amounts  $50\%$  or less of the ULS capacity of the connection.

This could be confirmed by investigations by Schaumann et al. [2]. In contrast to these results, Schaumann et al. [2] observed degradation processes of similar specimens tested in wet AC at load levels of 50 % and below.

Moreover, the investigations evaluated by Lochte-Holtgreven [17] were conducted at a loading frequency of  $f = 10$  Hz (cf. [16]), while the tests by Schaumann et al. [2] were tested at  $f = 5$  Hz. A comparison of these results suggests that the loading frequency has no influence on the fatigue performance of grouted joint specimens in dry AC, at least in this frequency range. Thus, a variation of the ambient condition can be excluded from the list of parameters for the factorial experiment. For the remaining parameters two values each have to be set as follows.

The first value for the maximum compressive load  $F_{max}$  is set to 50 % of the connection's ULS capacity  $F_{ULS}$ . This allows a direct comparison between the mentioned fatigue test results in dry AC and results for wet AC. The second value for  $F_{max}$  is chosen to be 20 %  $F_{ULS}$ . Since the prior investigations [2] revealed a low number of endurable load cycles  $N$  for the load level of 50 %, 20 % might lead to a significantly higher  $N$ . The lower bound of the applied load range is set to  $R = 0.05$ , which allows a good utilisation of the test rig capacity. According to Billington et al. [6], real grouted joints are loaded with a load relation of up to  $R = -0.5$ . Hence, the following results can be rated as non conservative regarding the applied stress range.

For the loading frequency  $f$  the first value is set to 5 Hz. This enables a good comparability to prior investigations (cf. [2], [16]). The main fatigue causing loads in real grouted joints act in the range of the structure's first eigenfrequency. For a jacket substructure this is about 0.3 Hz (cf. [20]). So, the second value for  $f$  is set to 1 Hz. This will give an insight on the effect of  $f$  on the fatigue performance while enabling economic testing times. The chosen input parameters are transferred into a factorial experiment chart given in Table 1, where each row represents one parameter combination.

Finally, a response variable has to be set for the experiment. Here, the usual response variable in fatigue tests, the number of endurable load cycles  $N$ , is chosen. The limit of durability is defined as a decrease of specimen stiffness within a small number of load cycles (cf. Figure 7, end of plot), followed by a total failure of the specimen. Additionally,  $N$  is limited to two million load cycles as maximum, similar to common fatigue tests (cf. [12]).

For each combination of parameters an amount of three test results is gathered. The mean value  $y_i$  and the variance  $s_i^2$  are calculated from these three results. Subsequently, the variances multiplied with the parameters' factors (-/+ ) are summed up  $|\Sigma|$  per parameter as well as interactions and their effect (EFF) is calculated. In conclusion the significance level (SIG) of each effect is determined in a student's t-test. Hence, the variation of all tested parameters is assumed to be normally distributed.

### 3 RESULTS AND DISCUSSION

#### 3.1 Material tests

Figure 5 shows the strength and stiffness properties of the two applied grout materials. The values include information from the official data sheets by the manufacturer (M) and independent material test results (B1-3) conducted by the Institute for Building Material Science (IfB). All values are mean values. Moreover, for the independent material tests, according to the amount of underlying results, the 95 % confidence interval is presented. Besides the materials uniaxial compressive strength  $f_c$ , its tensile strength  $f_t$  and its bending tensile strength  $f_{bt}$  are illustrated. Additionally, the material's elastic compressive modulus  $E_c$  and the ultimate capacity  $F_{ULS}$  of small scale grouted joint specimens are depicted.

For the outlined test results, material 1 shows a clearly higher  $f_c$  than stated by the manufacturer while material 2 is slightly weaker than stated by the manufacturer. Especially for the prism specimens, that have the highest amount of underlying results, the two materials seem to have almost identical  $f_c$ . Similar to that,  $f_t$  of material 1 is in the range of the manufacturer's data while for material 2  $f_t$  is clearly lower than stated by the manufacturer. Furthermore,  $E_c$  and  $F_{ULS}$  are in a

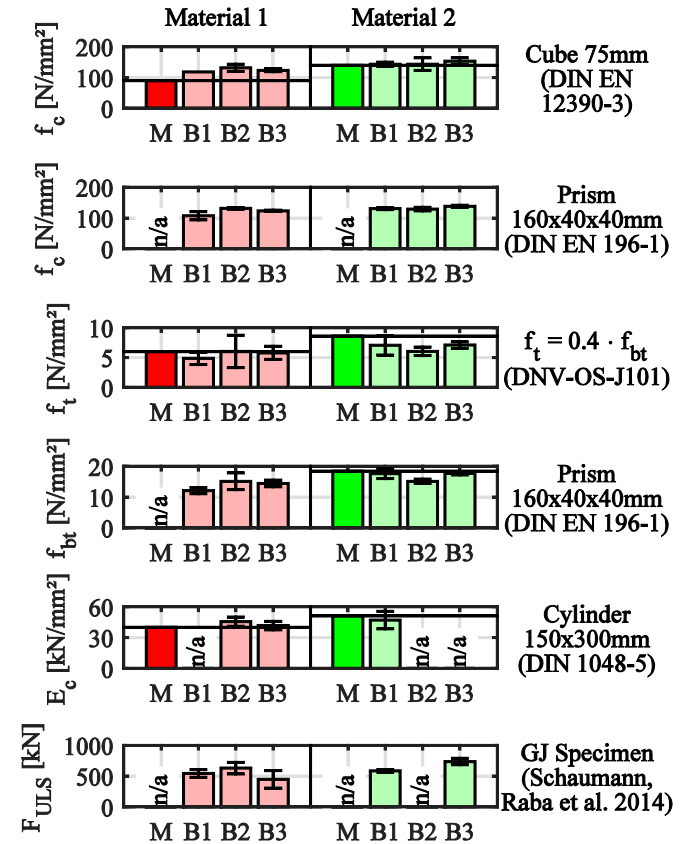


Figure 5: Strength and stiffness properties (28d values) with 95% confidence interval for the two applied grout materials (M: data provided by the manufacturer, B1-3: data from three different production batches determined by IfB and IfS)

similar range for both materials.

In general, many of the 95 % confidence intervals overlap between the two materials. Therefore, the effect of different grout material strengths is not representable by the small scale grouted joint specimens with the chosen grout materials. Both materials are too alike regarding their mechanical properties.

### 3.2 Factorial experiment

The results of the factorial experiment are given in Table 1. For parameter combinations 2-8 three tests each were conducted. Parameter combination 1 and 5 are the most time consuming combinations with about four weeks of testing time per specimen. Based on the results of parameter combination 3, 5 and 7, real tests for combination 1 were renounced and the results were estimated.

The maximum compressive load  $F_{max}$  has an effect on the results with significance of 99.9 %. With decreasing load level  $F_{max}$ , the number of endurable load cycles  $N$  increases. This result could be expected for fatigue tests since a lower load causes a lower stress state in the filling material.

The loading frequency  $f$  shows a similar result. With significance of 99.5 % a lower frequency leads to a higher number of endurable load cycles. As stated in section 2.4 this effect depends on the wet AC and will not appear with a similar significance for tests in dry AC. Schaumann et al. [2] described different effects of attrition, which are slowed down by a lower frequency and therefore lead to a higher  $N$ .

On the contrary, the two different grout materials have no significant effect on the test results, but this effect needs a closer look. As stated in Section 3.1 the applied grout materials show no significant strength difference. In addition,  $F_{max}$  is set in relation to  $F_{ULS}$  for each material batch. Thus, the influence of the material strength is excluded from the analysed results. As a consequence the material effect given in Table 1 might depend only on the material's microstructure or chemical properties. These properties were not investigated in the scope of this experiment.

The only significant interaction is between  $F_{max}$  and  $f$  with a significance of 99.5 %. A low  $F_{max}$  and a low  $f$  lead to the

highest  $N$ , while a high  $F_{max}$  and a high  $f$  result in the lowest  $N$ . This interaction can be explained by the effect of each parameter. A lower load  $F_{max}$  causes less deformation and therefore, a lower pumping velocity. For  $f$  the same effect occurs. In total these effects add up and are mutually reinforcing.

Furthermore, it is worth mentioning, that all resulting  $N$  for the lower load level of 20 %  $F_{max}/F_{ULS}$  are not defined by failure of the specimen, but by the cycle limit of the test procedure (cf. Section 2.4). Hence, it is recommendable to take a closer look at the specimens' deformations to evaluate effects on the fatigue performance.

### 3.3 Specimen deformation

Figure 6 shows a close up of the first load cycles of two small scale grouted joint specimens loaded at 50 %  $F_{max}/F_{ULS}$  and 20 %  $F_{max}/F_{ULS}$  with a loading frequency of 5 Hz each. Figure 7 shows that there is an initial displacement  $u_0$  that remains during further load cycles. This initial displacement occurs due to imperfections of the water basin floor (cf. Section 2.2) as well as initial settlements of the grout material in the contact interface. Its size differs for each specimen. To reduce this effect on the measurement data, the initial displacement for each specimen is determined and is subtracted from the measurement data. Since the initial phase is non-linear, the initial displacement  $u_0$  is defined as the zero crossing of the elastic secant  $K$  between  $F_{max}$  and  $F_{mean}$ . The elastic secant  $K$  is defined in the first cycle with full load range  $F_{max}-F_{min}$ .

The modified mean displacement  $u_{mean}$  of the three small scale grouted joint specimens per load level is presented in Figure 7. The upper plot shows the results for a load level of 50 %  $F_{max}/F_{ULS}$  while the lower plot shows the results for a load level of 20 %  $F_{max}/F_{ULS}$ .

For the higher load level the specimens' displacement increases within the first 5 % of endurable load cycles. After that, the displacement stabilizes but continues until the specimen loses its remaining stiffness within the last about 5 % of endurable load cycles. The specimens fail at a final displacement of about 6 mm.

Table 1: Factorial experiment chart with results and evaluation (values in brackets are estimated results)

No.	$F_{max}/F_{ULS}$ A - : 20 % + : 50 %	Frequency B - : 1 Hz + : 5 Hz	Material C - : Mat 1 + : Mat 2	Interactions				Result N [-]			$y_i$	$s_i^2$
				AB	AC	BC	ABC	1	2	3		
1	-	-	-	+	+	+	-	(2.00E+06)	(2.00E+06)	(2.00E+06)	(2.00E+06)	(0.00E+00)
2	+	-	-	-	-	+	+	1.03E+05	1.16E+05	8.02E+04	9.98E+04	3.36E+08
3	-	+	-	-	+	-	+	2.00E+06	2.00E+06	2.00E+06	2.00E+06	0.00E+00
4	+	+	-	+	-	-	-	6.41E+04	3.14E+04	3.53E+04	4.36E+04	3.20E+08
5	-	-	+	+	-	-	+	2.00E+06	2.00E+06	2.00E+06	2.00E+06	0.00E+00
6	+	-	+	-	+	-	-	1.12E+05	3.60E+04	1.25E+05	9.11E+04	2.31E+09
7	-	+	+	-	-	+	-	2.00E+06	2.00E+06	2.00E+06	2.00E+06	0.00E+00
8	+	+	+	+	+	+	+	3.07E+04	4.13E+04	4.20E+04	3.80E+04	4.01E+07
$ \Sigma $	7.73E+06	1.09E+05	1.43E+04	1.09E+05	1.43E+04	3.15E+03	3.15E+03				$\Sigma =$	3.01E+09
EFF	1.93E+06	2.73E+04	3.58E+03	2.73E+04	3.58E+03	7.89E+02	7.89E+02				$s^2 =$	3.76E+08
SIG	99.9%	99.5%	< 50.0%	99.5%	< 50.0%	< 50.0%	< 50.0%				$s_d =$	7.92E+03

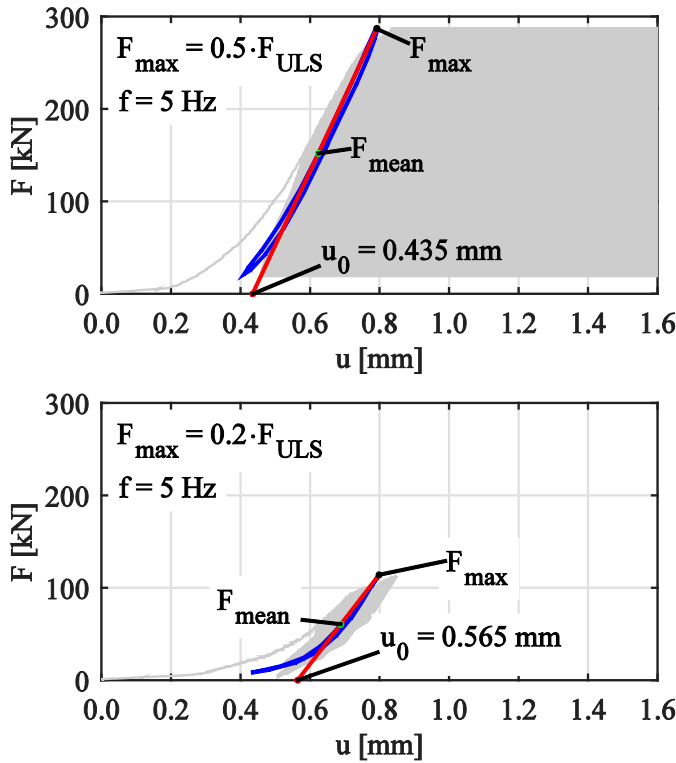


Figure 6: Force-displacement plot for two small scale grouted joint specimen, showing the initial displacement  $u_0$  due to specimen and test rig uncertainties

At the lower load level the specimens' displacement rises also within the first 5 % of endurable load cycles. Different to the higher load level, the displacement grows to a much higher amount. Afterwards, the specimens' displacement linearly increases until the load cycle limit of 2 million is reached. A third phase in which the specimens lose their remaining stiffness is not visible in the results. It should be emphasized, that the final mean displacement lies in the range of  $u_{\text{mean}} \sim 12$  and  $\sim 23$  mm.

According to the load bearing behaviour of the connection (cf. Section 1), the displacement influences the angle of the compression struts as well as which shear keys are involved. Figure 8 shows the occurring compression strut angles for different levels of displacement. The larger the relative displacement between pile and sleeve gets, the flatter the angle of the compression strut gets and the lesser vertical load can be transferred. As described by Krahl & Karsan [21], the local load application of the shear keys leads to high compressive stress in the grout. As a result, the grout material is crushed and a wedge of loose grout material occurs in front of the shear keys. For wet AC, the water washes out this loose material and the pile can lower down into the clearance. At the lower position of the pile, this process is repetitive until the transferable vertical load part of the compression strut is smaller than the applied load. At this point the connection fails. For the load level of 20%  $F_{\text{max}}/F_{\text{ULT}}$ , this intersection between

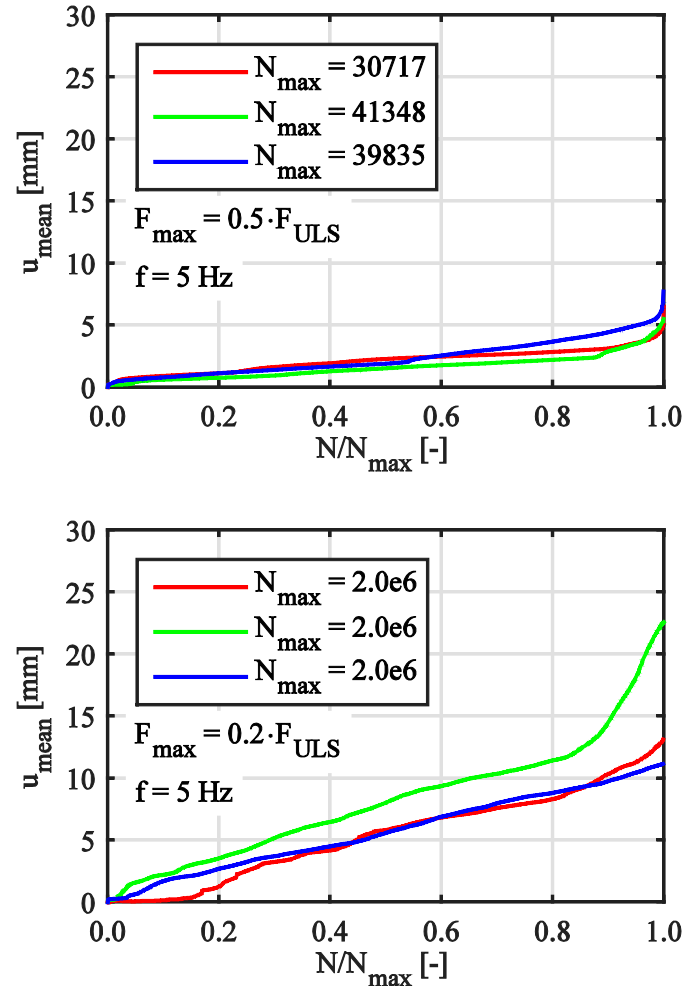


Figure 7: Modified mean displacement  $u_{\text{mean}}$  over number of normalized load cycles  $N/N_{\text{max}}$  for a small scale grouted joint specimen loaded at 50 %  $F_{\text{max}}/F_{\text{ULT}}$  (upper plot) and loaded at 20 %  $F_{\text{max}}/F_{\text{ULT}}$  (lower plot)

action and resistance seems not to be reached within the applied 2 million load cycles.

### 3.4 Stiffness degradation

In the previous section the load cycle dependent behaviour of the mean displacement of the small scale grouted joint specimen was described. Finally, a closer look shall be taken at the dynamic stiffness degradation. This means the stiffness within each load cycle being a measure for the size of the displacement range  $u_{\text{max}} - u_{\text{min}}$ . As described in section 3.3, the test results show an impact of the test rig deformations. Besides the mentioned initial displacement, a further effect is visible in Figure 9. In this figure the force-displacement dependency for the test rig with a steel dummy specimen is presented. It shows that for different load levels the non-linear stiffness of the test rig influences the measured specimen stiffness. The lower plot shows the dynamic stiffness  $K_{\text{dyn}}$  per load cycle, calculated with

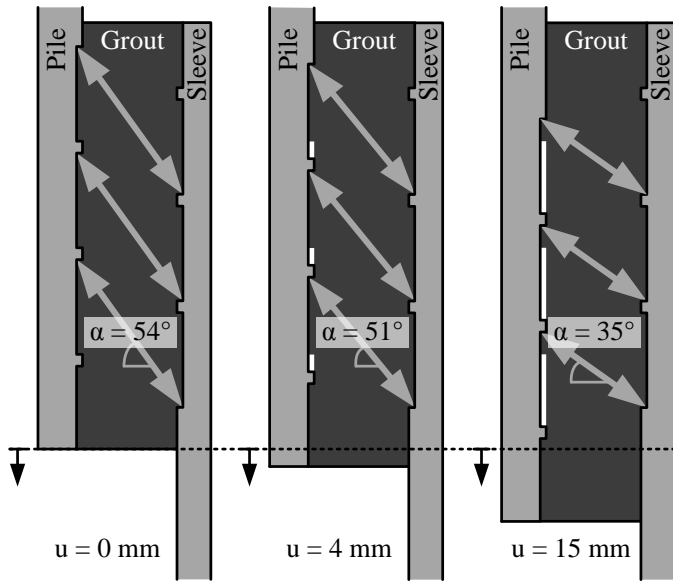


Figure 8: Displacement of the grouted joint parts of a small scale specimen and occurring compression struts for different displacements of the pile

$F_{max}$  and  $F_{min}$  ( $K_1$ , red line), with  $F_{max}$  and  $F_{mean}$  ( $K_2$ , green line) as well as their ratio ( $K_2/K_1$ , blue line).

At low load levels a large displacement occurs, which leads to almost horizontal hysteretic loops in the plot. From about 50 kN upwards, the displacement increase reduces distinctly and the hysteretic loops become steeper. This behaviour is also visible in the plots of the dynamic stiffness

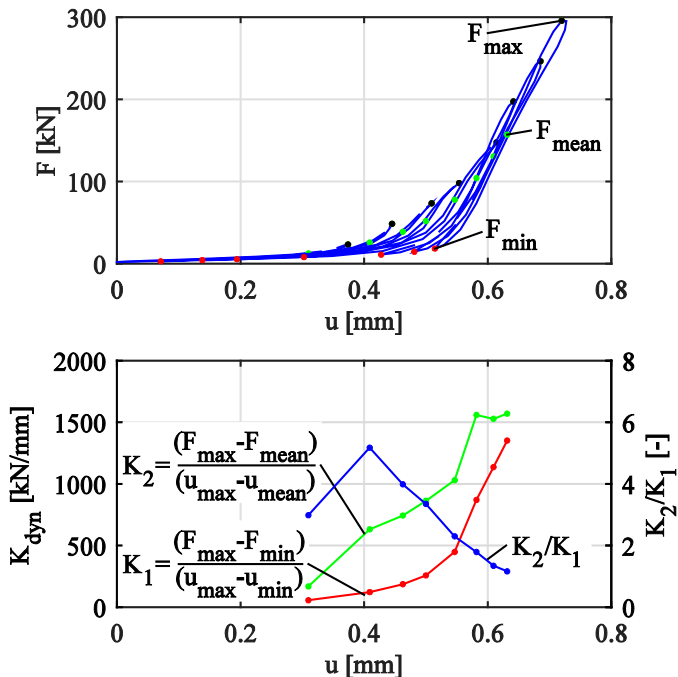


Figure 9: Force-displacement and stiffness-displacement plot for the fatigue test rig with a steel dummy specimen

$K_{dyn}$ . Since the lower load level  $F_{min}$  is related to the level of  $F_{max}$  by  $R = 0.05$ , for all conducted tests  $F_{min}$  is below 50 kN. Hence, calculating  $K_{dyn}$  with  $u_{min}$  ( $K_1$ , red line) leads to an underestimation of the specimen's stiffness. Certainly,  $u_{mean}$  lies out of the influence area of the test rig and calculating  $K_{dyn}$  with  $u_{mean}$  ( $K_2$ , green line) reduces the non-linear influence. As a result, from a load level of  $F_{max} = 200$  kN on the dynamic stiffness  $K_2$  seems to converge.

Figure 10 and Figure 11 show the force-displacement plots of every tenth of the total endurable load cycles  $N_{max}$ . For each hysteretic loop  $K_{dyn}$  is evaluated as described before and also plotted. In Figure 10 the results for the higher load level of 50 %  $F_{max}/F_{ULS}$  are illustrated and in Figure 11 the results for a load level of 20 %  $F_{max}/F_{ULS}$  are presented. The comparison between the  $K_{dyn}$  values shows that the non-linear influence decreases with higher load levels. This observation corresponds to the results for the steel dummy specimen measurement as shown in Figure 9. Moreover, the stiffness  $K_2$  is at a similar level of  $K_{dyn} \sim 750$  kN/mm for both loading situations. The slightly smaller  $K_{dyn}$  at the load level of 20 %  $F_{max}/F_{ULS}$  can be explained by the non-linear influence, still affecting the  $K_2$  stiffness due to the low load level. As a result, the stiffness of the specimen seems to be independent from the applied load level. Furthermore,  $K_{dyn}$  shows no clear degradation with increasing number of applied load cycles.

#### 4 CONCLUSIONS

Within this paper, the fatigue performance of small scale grouted joint specimens was investigated. Results of 24 specimens with identical geometry and two different filling materials were presented. The individual tests differed by means of the applied load level  $F_{max}/F_{ULS}$  and the loading frequency  $f$ . All tests were conducted in submerged conditions. For the varied parameters  $F_{max}/F_{ULS}$ , frequency and grout material, a factorial experiment was elaborated and the results were statistically evaluated. Moreover, a closer look was taken at the filling material properties, the specimens' deformation evolution over number of applied load cycles and the stiffness within single hysteretic loops.

The factorial experiment evaluation showed a high significance of the applied load level  $F_{max}/F_{ULS}$  and the loading frequency  $f$ . In addition, these parameters are significantly correlated. For the two chosen filling materials no significant effect could be determined.

The specimens' mean deformation  $u_{mean}$  over number of applied load cycles is governed by the wash out effects of the water. At low load levels large displacements are possible with preserving load bearing capacity. At high load levels the specimens fail within a small range of applied load cycles.

For the dynamic stiffness  $K_{dyn}$  no impact of the applied load could be detected. Furthermore,  $K_{dyn}$  shows no sign of degradation with increasing number of applied load cycles.

In conclusion, prior observations from submerged fatigue tests on small scale grouted joint specimens could be confirmed with the presented statistically secured results. The effects of attrition due to the surrounding water influence the cracking

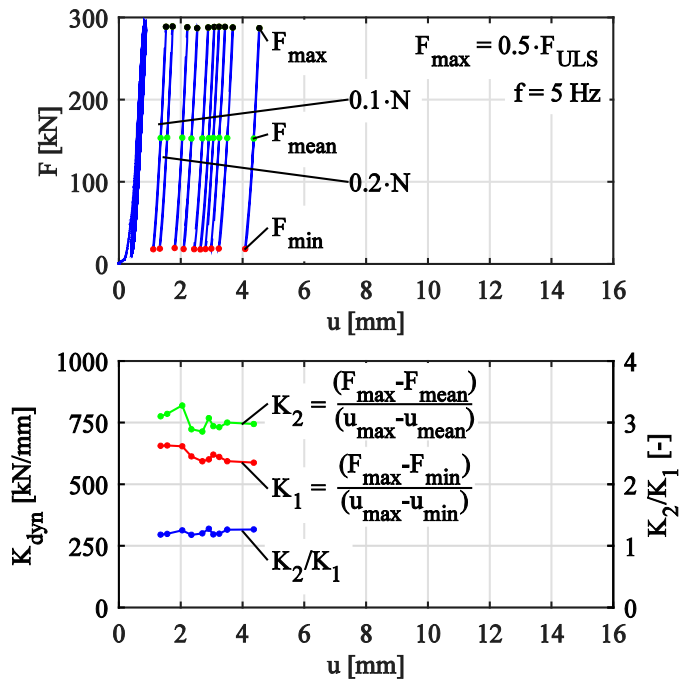


Figure 10: Force-displacement and stiffness-displacement plot for the fatigue test of a small scale grouted joint specimen loaded at 50 %  $F_{max}/F_{ULS}$  and with a frequency of 5 Hz

behaviour and the volume of the grout. As a result, for the presented pure compression tests, the water effect is most clear by the evolution of the mean displacement  $u_{mean}$ . Subsequently, this influences the number of endurable load cycles  $N$ .

Future small scale grouted joint fatigue tests will focus on the influence of the loading frequency. Besides, submerged large scale grouted joint fatigue tests with full load reversal will be conducted. These tests will give insights on the transferability of the described effects of water to real grouted joints of offshore wind turbine structures.

#### ACKNOWLEDGMENTS

The presented results are achieved within the research project ‘GROWup – Grouted Joints for Offshore Wind Energy Converters under reversed axial loadings and up scaled thicknesses’ (funding sign: 0325290) funded by the German Federal Ministry for Economic Affairs and Energy (BMWi). The research partners are Institute for Steel Construction and Institute of Building Materials Science, both at Leibniz University Hannover, Germany. The authors thank the BMWi for funding and all accompanying industry project partners (Fraunhofer IWES, DNV GL, Senvion, RWE Innogy, STRABAG) for their support. In addition the authors thank the material manufacturers for their free material supply.

#### REFERENCES

[1] Lamport W. B., 1988: "Ultimate Strength of Grouted Pile-to-Sleeve-Connections". Dissertation, University of Texas at Austin, Austin, Texas, USA.

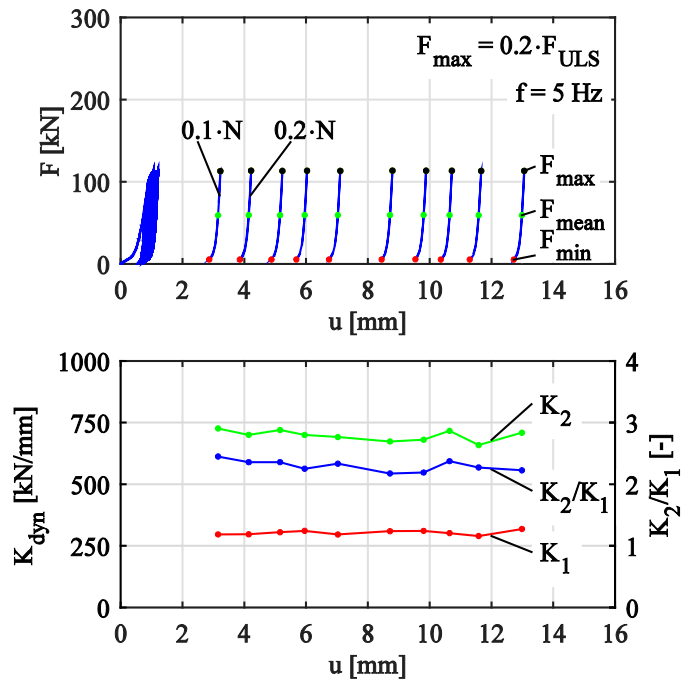


Figure 11: Force-displacement and stiffness-displacement plot for the fatigue test of a small scale grouted joint specimen loaded at 20 %  $F_{max}/F_{ULS}$  and with a frequency of 5 Hz

[2] Schaumann P., Raba A., and Bechtel A., 2014: "Effects of Attrition Due to Water in Cyclically Loaded Grouted Joints". *Proceedings of the ASME 2014 33rd International Conference on Ocean, Offshore and Arctic Engineering*, San Francisco, California, USA.

[3] DIN EN ISO 19902, January 2014: "Petroleum and Natural Gas Industries – Fixed Steel Offshore Structures (in German)". DIN Deutsches Institut für Normung e.V.

[4] Billington C. J., and Tebbet I. E., 1982: "Fatigue of grouted connections". *Proceedings of the IABSE Colloquium Lausanne: Fatigue of Steel and Concrete Structures*, pp. 625–632, Lausanne, Swiss.

[5] Harwood R. G., Billington C. J., Buitrago J., Sele A. B., and Sharp J. V., 1996: "Grouted Pile to Sleeves Connections: Design Provisions for the New ISO Standard for Offshore Structures". *Proceedings of the ASME 1996 15th International Conference on Ocean, Offshore and Arctic Engineering*, Florence, Italy.

[6] Billington C. J., and Chetwood J., 2012: "Lessons from Previous Research for the Design of Grouted Connections for Offshore Wind Foundations: A New Interpretation". *Proceedings of the International Quality & Productivity Center Conference*.

[7] DNV-OS-J101, May 2014: "Design of Offshore Wind Turbine Structures". Det Norske Veritas.

[8] Waagaard K., 1977: "Fatigue of Offshore Concrete Structures: Design and Experimental Investigations". *9th Annual Offshore Technology Conference*, pp. 341–350, Houston, Texas, USA.

- [9] Waagaard K., 1986: "Experimental Investigation on the Fatigue Strength of Offshore Concrete Structures". *9th Annual Energy Technology Conference*, pp. S. 73-81, New Orleans, Louisiana, USA.
- [10] Nishiyama M., Muguruma H., and Watanabe F.: "On the Low-cycle Fatigue Behaviours of Concrete and Concrete Members under Submerged Condition". 1987.
- [11] Nygaard K., Petkovic G., Rosseland S., and Stemland H., 1992: "High Strength Concrete, SP3 - Fatigue: Report 3.1: The Influence of Moisture Conditions on the Fatigue Strength of Concrete". SINTEF Structural Engineering - FCB, Trondheim, Norway.
- [12] Soerensen E. V., 2011: "Fatigue Life of High Performance Grout in Dry and Wet Environment for Wing Turbine Grouted Connections". *Proceedings of the European Windenergy Association Offshore Conference EWEA Offshore 2011*, Amsterdam, Netherlands.
- [13] Schaumann P., Raba A., and Bechtel A., 2013: "Impact of Contact Interface Conditions on the Axial Load Bearing Capacity of Grouted Connections". *Proceedings of the European Windenergy Association Conference EWEA 2013*, Vienna, Austria.
- [14] Schaumann P., and Wilke F., Fatigue Assessment of Support Structures of Offshore Wind Energy Conversion Systems, *Annual Report 2005*, pp. 36–39, Schaumann P., and Peinke J., eds., Hannover, Germany, 2006.
- [15] Anders S., 2007: "Betontechnologische Einflüsse auf das Tragverhalten von Grouted Joints" (Influences of Concrete Technology on the Bearing Behaviour of Grouted Joints). Dissertation, Institute for Building Materials Science, Leibniz University Hannover, Hannover, Germany.
- [16] Schaumann P., Keindorf C., and Lochte-Holtgreven S.: "Statische und dynamische Axialdruckversuche an vergROUTETEN Rohr-in-Rohr-Verbindungen mit verschiedenen Füllmaterialien" (Static and Dynamic Axial Compression Tests on Grouted Tube-in-Tube Connections with Various Grout Materials). *Bautechnik*, **86**(11), pp. 719–728, 2009.
- [17] Lochte-Holtgreven S., 2013: "Zum Trag- und Ermüdungsverhalten biegebeanspruchter Grouted Joints in Offshore-Windenergieanlagen" (On Load Bearing and Fatigue Behaviour of Grouted Joints in Offshore Wind Turbines Subjected to Bending). Dissertation, Institute for Steel Construction, Leibniz University Hannover, Hannover, Germany.
- [18] Wilke F., 2014: "Load Bearing Behaviour of Grouted Joints Subjected to Predominant Bending". Dissertation, Institute for Steel Construction, Leibniz University Hannover, Hannover, Germany.
- [19] Kleppmann W., 2011. *Taschenbuch Versuchsplanung: Produkte und Prozesse optimieren*, 7th ed., Hanser, München.
- [20] Schaumann P., Böker C., and Wilke F.: "Lebensdaueranalyse komplexer Tragstrukturen unter Seegangsbeanspruchung" (Life Cycle Analysis for Complex Substructures in Maritime Loading). *Stahlbau*, **74**(6), pp. 406–411, 2005.
- [21] Krahl N. W., and Karsan D. I.: "Axial Strength of Grouted Pile-to-Sleeve Connections". *Journal of Structural Engineering*, **111**(4), pp. 889–905, 1985.